Chemistry Europe
European Chemical Societies Publishing

Rigidly Fused Spiro-Conjugated π-Systems

Shihui Liu,[a] Debin Xia,*[a] and Martin Baumgarten*[b]

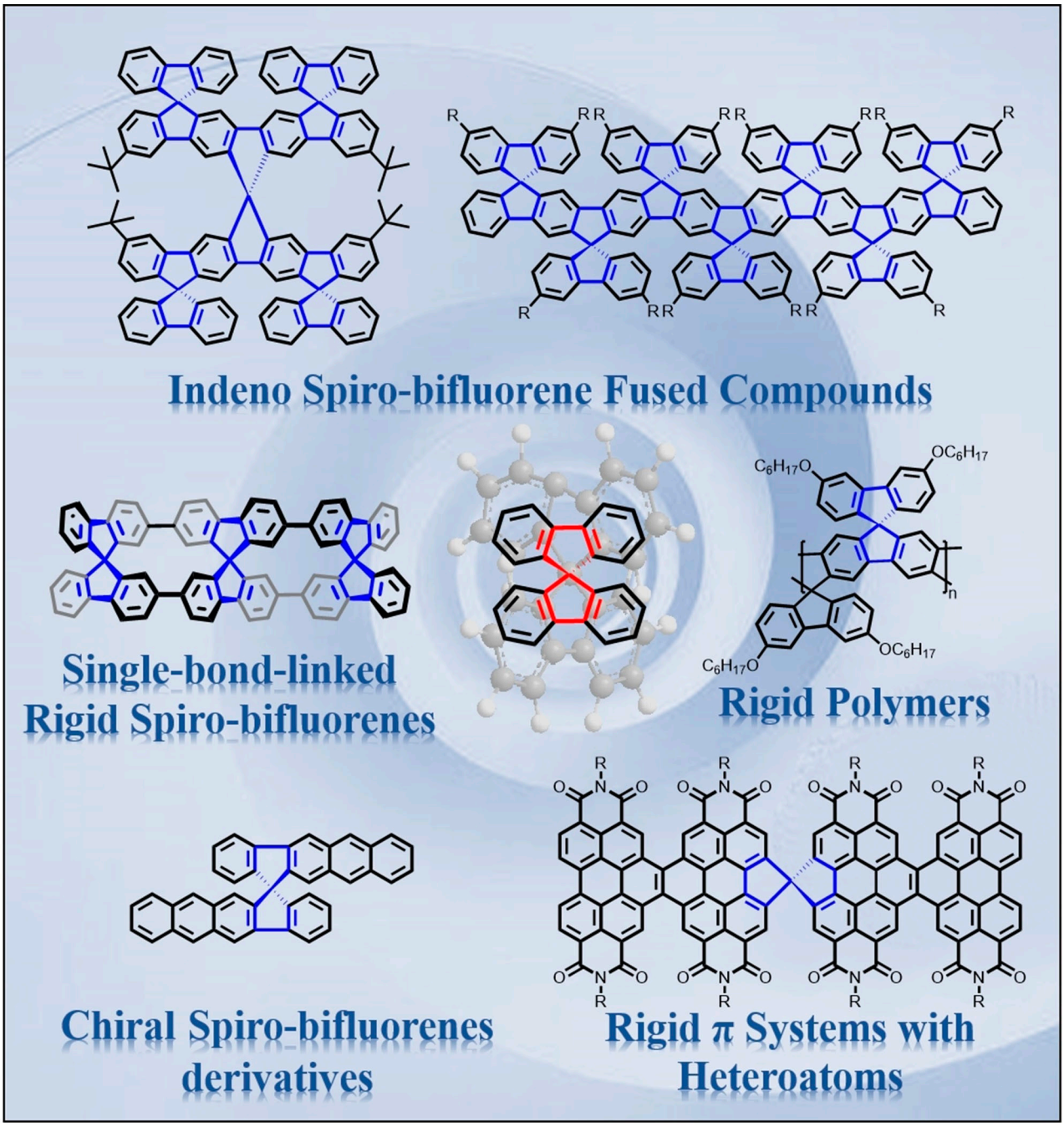

Spiro-fused π-systems have gained considerable attention for their application as semiconductors in molecular electronics. Here, a synopsis regarding recent breakthroughs in ladderized spirobifluorenes and indeno-spirobifluorenes, along with further spiro-condensed heteroatomic hydrocarbons with donor-acceptor moieties, is provided. Additionally, an extended range of rigid spirobifluorene polymers and specific doubly linked spiro-systems with partial chiral character is discussed. The diverse applications of the aforementioned structures are thoroughly evaluated.

1. Introduction

Orthogonally conjugated π-systems are commonly viewed as disconnected, due to π-overlaps being hindered by 90° angles. The conjugation of spiro compounds, particularly spirononatetraene, has been historically and scientifically disputed; therefore, the term spiro-conjugation was established.[1] These conjugations, however, overlap between adjacent chromophores by an insignificant margin, as indicated by their minor red shift when compared with the isolated sub-molecular entities.

Spirobifluorene compounds can be considered as two planarized biphenyl bodies linked through a tetragonal carbon center, resulting in a cross-type structure. Common applications include their utilization as components in organic electronics, such as organic light emitting diodes (OLED),[2–8] organic field effect transistors (OFETs),[2,4] and organic solar cells (OSCs).[2,4, 9–13] Linkages between spirofluorenes typically comprise of single bonds or flexible segments, occasionally inducing bond rotations, which might lead to undesirable nonradiative decay, large Stokes shifts, and low thermal stability. Considering the prominent role of spirolinked π-systems in organic electronics, the discovery of rigidly fused spirocycles is highly important.

Furthermore, spiro-fusion with donors and/or acceptors can potentially augment the dimensionality of conjugated molecules and polymers (which commonly are linear quasi-one-dimensional systems with 2D and/or 3D structural motifs). In this review, we summarized the primary aspects of rigidly fused spiro-conjugated π-systems, such as their synthetic strategies and physical-chemical properties (both in chemical solutions and in their solid amorphous and crystalline state), as well as their structural description and device performances.

2. All carbon spiro-bifluorene and indeno spiro-bifluorene-fused compounds

The dispiro[fluorene-9,6-indeno[1,2-b]fluorene-12,9′-fluorene] (**1**) that structurally combines dihydroindenofluorene and spirobifluorene was reported by Rault-Berthelot's et al.[14] Compared with blue-emitting units, such as fluorene and spirobifluorene, the photoluminescence quantum yield (PLQY) of compound **1** was enlarged by 150 and 7.5 times, respectively, under the same conditions. Intriguingly, high-yield formation of insoluble transparent polymer films was induced by electrochemical oxidation on the electrode surface. Subsequently, compound **1** was synthesized with varying substituted groups at different positions (Scheme 1). Compounds **2**[15] **3**[16] and **4**[17] exhibited considerably comparable fluorescence spectra, with emission peaks at approximately 348 nm and 370 nm, respectively. The emission bands of compounds **5**, **6**, and **7**, sustained bathochromic shifts (unlike **1**) due to the extended π-conjugation effect.[18] Compound **4** with *tert*-butyl groups (^{t}Bu) possessed a notable PLQY of 70%. The quantum yield was not further enhanced by the substitution of fluorene rings with phenyl arms in compounds **5**–**7**, and remained at ~75%. Additionally, the emission spectra of compounds **5**–**7** were redshifted as a result of the varying substituted moieties.

In 2007, Bo et al. conducted a milestone research related to monodisperse spiro-bridged ladder-type oligo-phenylenes.[15] Compounds **2**, **8**, **9**, and **10** (Scheme 2) exhibited well-resolved absorption and emission spectra. As the length of the conjugated backbone increased, every absorption and emission peak was significantly redshifted. Ladder-type oligomers possess severe rigidity, which resulted in the negligible Stokes shifts of oligomers **2** (4 nm), **8** (5 nm), **9** (3 nm), and **10** (6 nm)

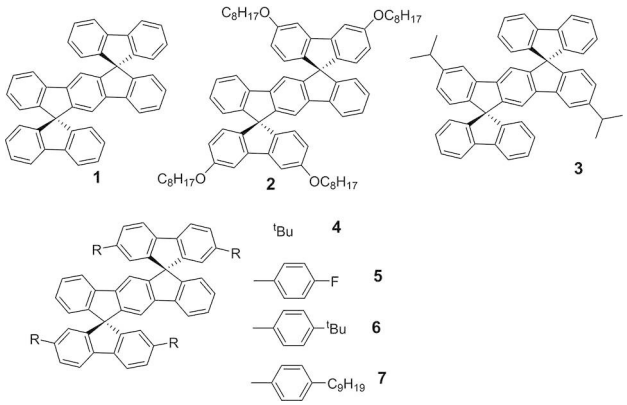

Scheme 1. Chemical structures of 6,12-dihydroindeno[1,2-b]fluorene and its derivatives.

[a] *S. Liu, Prof. Dr. D. Xia*
MIIT Key Laboratory of Critical Materials Technology for New Energy Conversion and Storage
School of Chemistry and Chemical Engineering
Harbin Institute of Technology, 150001 Harbin (P. R. China)
E-mail: xia@hit.edu.cn
[b] *Prof. Dr. M. Baumgarten*
Max Planck Institute for Polymer Research
Ackermannweg 10, 55128 Mainz (Germany)
E-mail: martin.baumgarten@mpip-mainz.mpg.de

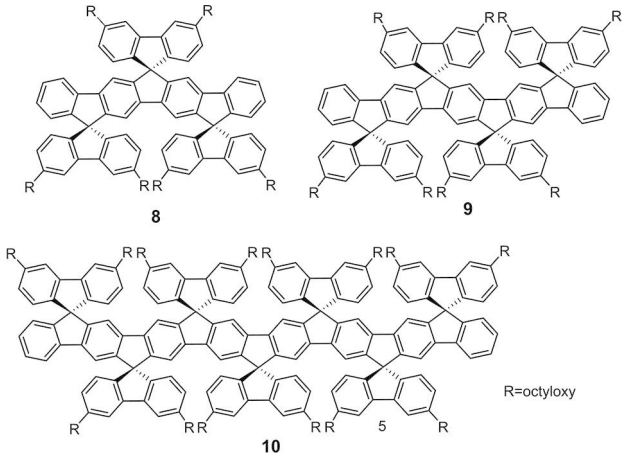

Scheme 2. Chemical structures of **8**–**10** with spirobridge and oligo-phenylenes.

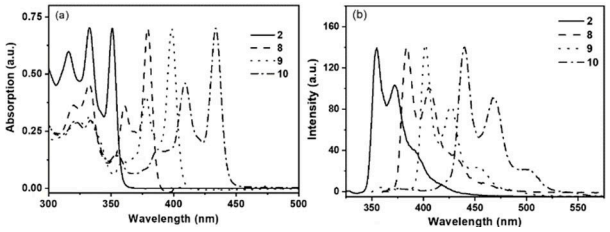

Figure 1. The absorption (a) and emission spectra (b) of compounds **2**, and **8**–**10**. Reproduced from reference [15] with permission from the American Chemical Society.

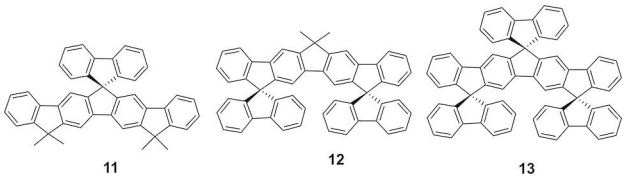

Scheme 3. Chemical structures of compounds **11**–**13** with the same bisindeno-fused fluorene backbone.

shown in Figure 1. It should be noted that nonradiative decay pathways were considerably inhibited in such spiro-fused oligomers, resulting in high PLQYs. Surprisingly, the PLQY of compound **9** in toluene solution approached 100%. Furthermore, the authors discovered that the highest occupied molecular orbitals (HOMO) of oligomers were enhanced in energy as the conjugation length increased, whereas the lowest unoccupied molecular orbitals (LUMO) declined. To our knowledge, compound **10** is the largest and most well-defined rigid ladderized phenylene molecule based completely on spirobifluorene, until now.

To promote vacuum process ability and single crystal growth, Hecht et al. explicitly omitted solubilizing groups.[19] Accordingly, compounds **11**, **12**, and **13** (Scheme 3) with methyl or spiro-fused fluorene were designed and synthesized. Single crystals from these three compounds were easily obtained through solution crystallization, or sublimation; however, the disparate crystal growth methods resulted in different crystal structures for compound **12** and **13** molecules. No direct π-stacking was observed in any of the three molecules. It was detected that every additional fluorene spiro-linkage to the conjugated backbones of compounds **11**–**13**, led to an approximate 2 nm redshift in the absorption and emission maxima peaks.

In 2008, Poriel et al. reported a ladder-type phenylene (namely compound **14**, Scheme 4) with a rigid backbone.[20] Single crystals of compound **14** were obtained through the solution evaporation method, possessing a conjugated backbone length of 19.4 Å (Figure 2A), and characterized by a non-

Shihui Liu received her bachelor's degree from Harbin University of Science and Technology in 2017 and her master's degree from Harbin Institute of Technology (HIT) in 2019. Now, she is a PhD student under the supervision of Associate Professor Debin Xia and Professor Sue Hao in HIT. She is currently working on the design and synthesis of thiophene-based polycyclic aromatic hydrocarbons and their applications in organic field-effect transistors.

Debin Xia received a bachelor's degree (2008) and a master's degree (2011) from Heilongjiang University under the supervision of Prof. Hui Xu, Prof. Zhengyu Yue, and Prof. Lixiang Wang. He then joined the group of Prof. Klaus Müllen at the Max Planck Institute for Polymer Research (MPIP) and obtained his PhD degree in December 2015. After that, he joined the Harbin Institute of Technology and currently serves as an Associate Professor in the School of Chemistry and Chemical Engineering. His research interests are in the synthesis and applications of polycyclic aromatic hydrocarbons.

Martin Baumgarten received his Ph.D. degree in 1988 from the Free University in Berlin under the supervision of Professor W. Lubitz. He was a postdoctoral researcher with Professor G. C. Dismukes at Princeton University (USA) before joining the group of Prof. K. Müllen at the Max Planck Institute for Polymer Research in Mainz (1990). In 1996 he received the venia legendi (habilitation) in Organic Chemistry at Johannes Gutenberg-University in Mainz. In 2001/2002 he was part time guest Professor at University of Saarland in Saarbrücken. His primary interest focuses on the design and synthesis of conjugated building blocks (oligomers and polymers) as semiconductors for molecular electronics, polyphenylene dendrimers, and stable organic high-spin molecules and molecular magnets as organic and hybrid spin networks.

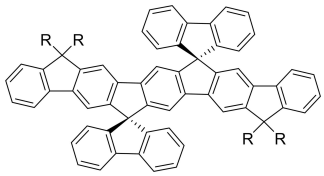

14

Scheme 4. Chemical structure of compound **14** (R = C_8H_{17}).

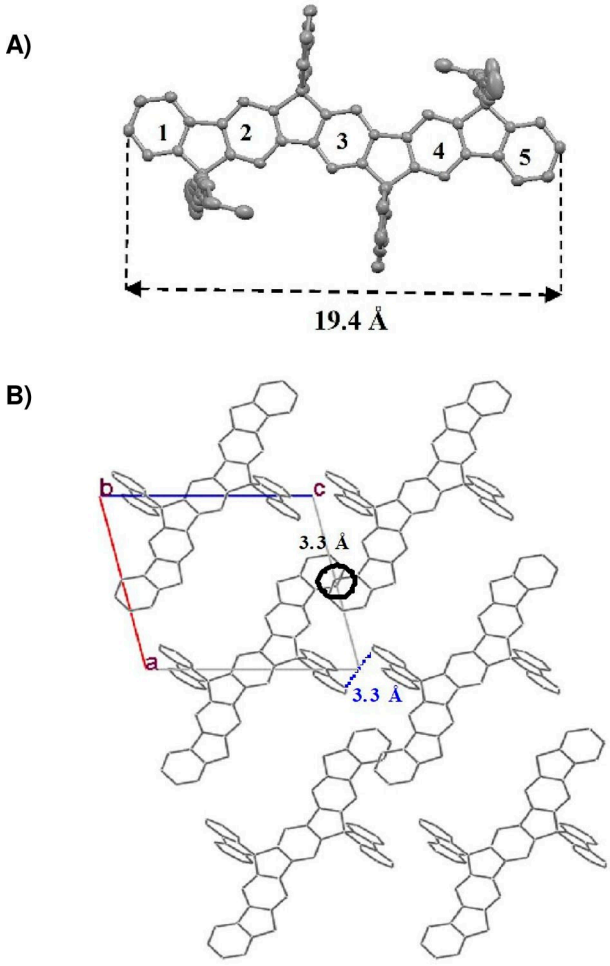

Figure 2. The molecular structure and crystal-packing diagram of compound **14**. The alkyl chains and hydrogen atoms have been omitted for clarity. Reproduced from reference [20] with the permission of Wiley-VCH.

flat backbone plane. No effective interchromophore π–π interactions in the solid state were shown in the packing diagrams. The closest C–C distance between two consecutive terminal phenyl rings of the backbone was estimated to be 3.3 Å (Figure 2B), which is the closest C–C distance between the substituted fluorene units of two adjacent molecules (dashed line).

Due to the extended conjugated backbone, the emission maxima of compound **14** were recorded at 397 and 420 nm, indicating a redshift compared with compound **1** (347 and 366 nm).[16] The PLQY of compound **14** in solution was 90%, substantially higher than compound **1** (62%), indicating that non-radiative decay pathways are less favorable. A combination of thin-film fluorescence spectra and thermal stress studies, however, indicated the chemical degradation of alkyl groups at the bridges of compound **14**, which caused the eminent low-energy emission. Low-energy emission was not observed in compound **1** under the same experimental conditions.

In 2019, 3D spiro-fused rigid compound **15** (Scheme 5) was prepared by Xia et al. with an overall yield of 88%.[21] Its *tert*-Butyl groups and 3D geometry enhanced its solubility in common organic solvents. The two diindeno-fused fluorene backbones spread over 15 Å in length and were perpendicular to each other (Figure 3), despite the annulated rigid and strained five-membered rings preventing the backbones from being completely flat. Two face-to-face fluorenes, standing at 8.76 Å apart, were quasi-parallel. No intermolecular π–π interactions were detected in the crystal packing diagram. The PLQY of compound **15** was measured at an exceptional 76%, indicating its optimal application in OLEDs. Finally, apart from

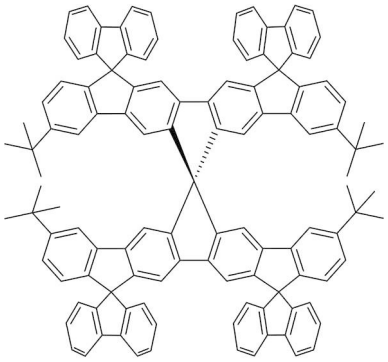

15

Scheme 5. Chemical structure of compound **15**.

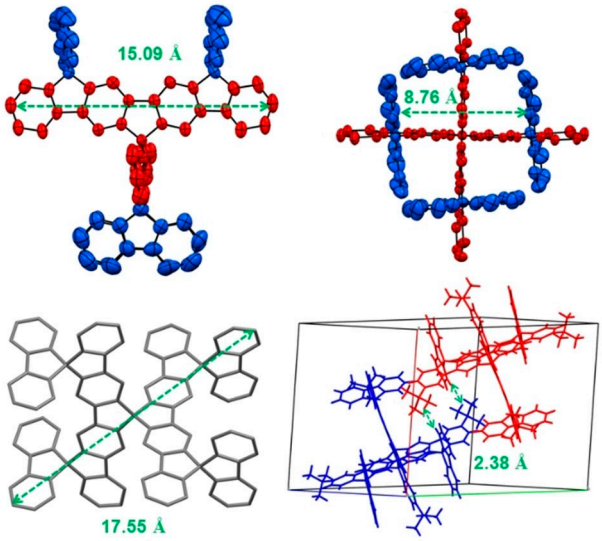

Figure 3. X-ray diffraction structure of compound **15**. *tert*-Butyl groups are omitted for clarity. Reproduced from reference [21] with permission from the Royal Society of Chemistry.

serving as an active component of blue OLEDs, compound **15** could be applied as a host for white OLEDs. In combination with the yellow emitter 3,4,5,6-tetrakis(3,6-diphenyl-carbazol-9-yl)-1,2-dicyanobenzene (4CzPNPh), white OLEDs are capable of offering a turn-on voltage of 3.5 V and a current efficiency (CE) of 3.6 Cd A^{-1}, along with CIE coordinates of (0.29, 0.33).[21]

Regarding the spiro-fused dihydroindenofluorene family, Poriel et al. systematically investigated four positional isomer compounds (**16**–**19**, Scheme 6) with three different phenyl linkages (para/meta/ortho), and two different ring bridge arrangements (anti/syn).[3,22–24]

As shown in Figure 4, compounds **1** and **16**–**19** displayed very similar low-energy absorption edges in THF solution, whereas their band intensities were significantly different. Compared with compounds **1**, **16**, and **17**, isomers **18** and **19** possessed weak low-energy absorption bands, caused by the highly distorted dihydroindenofluorene backbones. Time-dependent density functional theory (TD-DFT) simulations further confirmed the HOMO–LUMO transitions of compounds **18** and **19** to possess weak oscillator strengths (0.0231 and 0.0291),

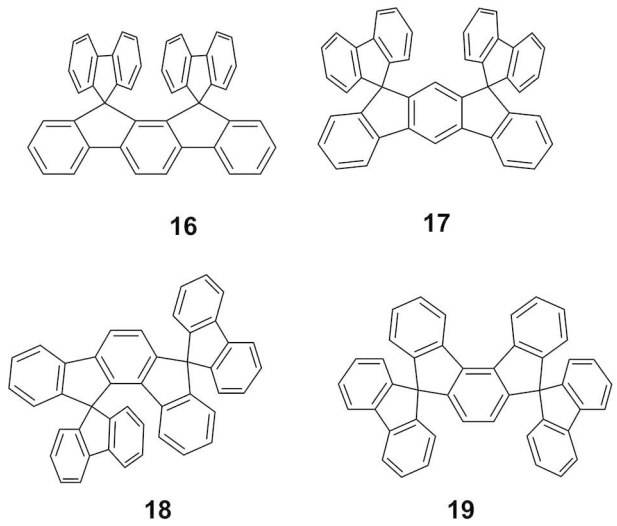

Scheme 6. Chemical structures of dihydroindeno-spirobifluorenes compounds **16**–**19**.

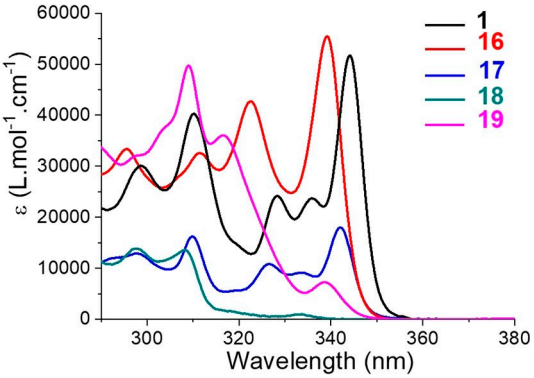

Figure 4. UV – vis absorption spectra of compounds **1**, and **16**–**19** in THF. Reproduced from reference [3] with permission from the American Chemical Society.

with the major π–π* transitions shifting to higher energies. Compared with all isomers, the PLQY of compound **18** was interestingly recorded at 23%, which was significantly lower than its isomers **1** (0.62), **16** (0.60), **17** (0.54), and **19** (0.50). Among the five isomers, compound **18** demonstrated relatively high triplet energy (2.76 eV), and thus was employed as a host for phosphorescent iridium complexes ($Ir(ppy)_3$, $E_T = 2.42$, FIrpic, $E_T = 2.64$ eV).[23] The green (or sky-blue) OLEDs presented a maximum CE of 57.3 cdA^{-1} (21.1 Cd A^{-1}), a maximum PE of 30.3 Lm W^{-1} (11.9 Lm W^{-1}), and external quantum efficiency (EQE) of 14.8% (7.5%).[23] Cyril Poriel et al. modified the structure of compound **16** by introducing varying aryl substitutes, which interestingly presented remarkable excimer emissions through intramolecular π–π interactions in the excited state, caused by the particular geometry.[25]

Stimulated by Poriel et al., Xia et al.[26] reported a multiple-spirobifluorene constructed blue emitter **20** with 3D geometry (Scheme 7), which exhibited a maximum decomposition temperature of 450 °C with 5% weight loss. The UV–vis absorption and emission spectra of compound **20** (in CH_2Cl_2) were very similar to those previously observed in its equivalents (**1**, **16**, **17**). However, compound **20** presented a relatively low PLQY of 45%, which could be attributed to the employment of varying standard references for PLQY measurement. Compound **20** was used as a host for the 3,4,5,6-tetrakis(3,6-diphenyl-carbazol-9-yl)-1,2-dicyanobenzene yellow emitter. The device showed a maximum CE, maximum PE, and EQE of 32.5 Cd A^{-1}, 15.3 Lm W^{-1}, and 11%, respectively.

3. Other extensions of condensed spirobifluorenes

In 2016, Parthasarathy and Jagarpu[27] reported the synthesis of π-expanded soluble 3D spirobifluorenes (compounds **21** and **22**, Scheme 8), which were obtained via an oxidative cyclization method utilizing DDQ/$MeSO_3H$ (rather than $FeCl_3$, which may result in chloro-**21** and chloro-**22**). The thermal decomposition temperatures of both compounds exceeded 450 °C. Spiro compounds **21** and **22** exhibited higher PLQYs than their (20,20-dihexyl-20H-cyclopenta[1,2-b:3,4-b′]ditriphenylene) planar counterparts. It should be noted that PLQY of film (0.86) of **21** remains almost the same as that of its toluene solution

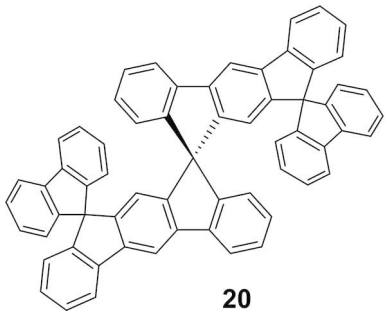

Scheme 7. Chemical structure of compound **20**.

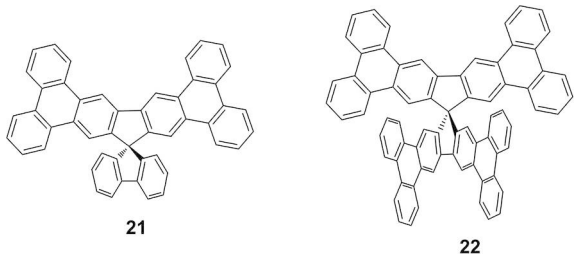

Scheme 8. Chemical structures of compounds **21** and **22**.

(0.84), whereas the PLQY of the compound **22** film increased drastically (solution PLQY = 78%; film PLQY = 88%). Compound **21** could further act as an excellent fluorescent sensor for nitroaromatic explosives with a detection limit up to 0.2–2.0 ppb.[27]

Harada et al.[28] designed and synthesized optically active spirobifluorene derivatives, namely compounds **23** and **24** (Scheme 9), which possessed two condensed anthracene and two naphthalene chromophores, respectively. By applying the CD exciton chirality method, their absolute stereostructures were unambiguously determined to be of the R type.

Further spiro-fused rigid molecules were synthesized, such as compounds **25**,[29] **26**[30] **27**,[30] and **28**[31] (Scheme 10), which are exceptional blue emitters that can serve both as structure modulation cores and host materials, in order to achieve the desired emitting properties. For instance, the PLQY of compound **28** reached up to 61%. When used in a non-doped

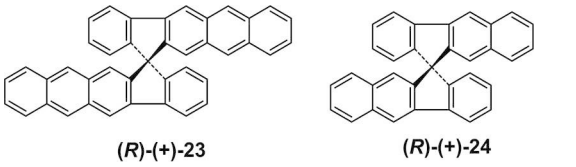

Scheme 9. Chemical structures of compounds **23** and **24**.

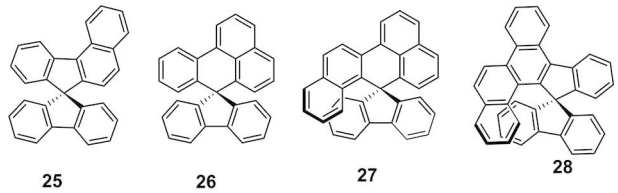

Scheme 10. Chemical structures of compounds **25**–**28**.

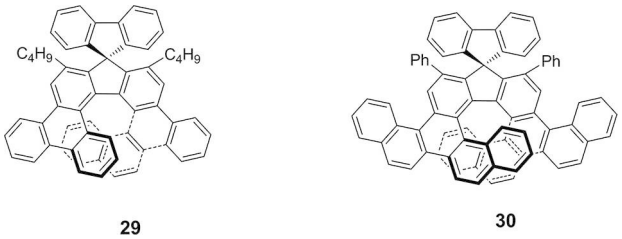

Scheme 11. Chemical structures of compounds **29** and **30**.

OLED, a CE of 1.21 Cd A^{-1}, PE of 0.70 Lm W^{-1}, and an EQE of 3.01% were achieved. A CIE of (0.153, 0.050) and an electroluminescence maximum wavelength of 435 nm were provided, indicating a deep-blue emission.

Tanaka et al. reported two helically chiral spiro-fused molecules **29**[32] and **30**[33] (Scheme 11). Both compounds exhibited circularly polarized luminescence properties. Compound **30** presented apparently redshifted absorption and emission maxima in comparison with the corresponding triphenylene-based compound **29**. The PLQY (18%) and optical rotation value (322) of helical compound **30**, however, were lower than triphenylene-based helical compound **29** (PLQY: 30%, optical rotation value: 684).

In 2016, Jin et al. developed a highly efficient $FeCl_3$-mediated oxidative spirocyclization of 1,2-di(9H-fluoren-9-ylidene)-1,2-diphenylethanes.[34] A new class of di-spirolinked indeno-[2,1-a]indene p-conjugated compounds, such as **31** (Scheme 12), were synthesized. The UV-vis absorption spectrum of compound **31** is highly comparable to compound **1**, as reported by Poriel and Rault-Berthelot et al.[14] However, compound **31** possessed reduced structural rigidity and a larger Stokes shift (15 nm), compared with compound **1** and its equivalents **16**–**20**. Recently, Nakamura et al. reported the axially chiral spiro-conjugated carbon-bridged p-phenylenevinylene compound **32**,[35] (Scheme 12) which exhibited a PLQY of 74% and a decomposition temperature of 335 °C (with 5% weight loss). More importantly, a series of compound **32** derivatives with four diarylamine units were efficiently obtained with a higher than 60% yield, which presented a low hole mobility of 3.84×10^{-5} $cm^2V^{-1}s^{-1}$; highly comparable with the most widely used hole-transporting material: 2,2′,7,7′-tetrakis (N,N-bis(p-methoxy-phenyl)amino)-9,9′-spirobifluorene (spiro-OMeTAD).[35]

Trispirocyclic hydrocarbon compound **33** (Scheme 13), possessing three 9-fluorene moieties around the core of truxene, was synthesized via truxenone with 2-bromobiphenyl coupling.[36] Compound **33** is a colorless solid, sparingly soluble in common organic solvents, and has a melting point of 500 °C. It was used as a core to construct highly stable blue light-emitting materials[37] and hole-transporting materials for OLEDs.[36]

Hexa-peri-hexabenzocoronene (HBC), with a pronounced self-assembly and high intrinsic charge-carrier mobility, has

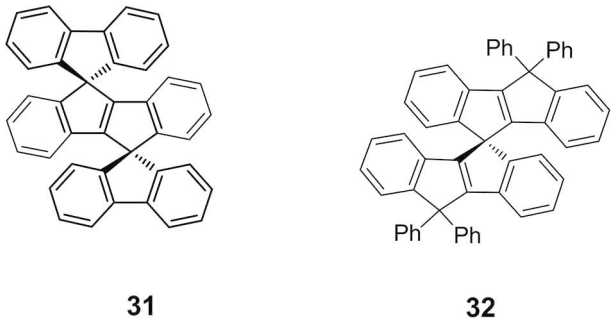

Scheme 12. Chemical structures of compounds **31** and **32**.

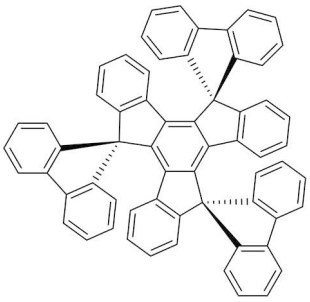

33

Scheme 13. Chemical structure of compound **33**.

been reported by Muellen et al.[38] This group has further demonstrated the efficient synthesis of a spiro-fused HBC dimer (compound **35**, Scheme 14) with robust orthogonally arranged spiro-linked HBC structures.[39] Noteworthily, adjacent compound **35** molecules are stacked by π–π overlaps of HBC subunits, with intermolecular distances ranging from 3.42 to 3.63 Å (Figure 5). Compared with its HBC counterpart, compound **35** exhibited a similar but less structured absorption pattern, along with a two-fold enhanced absorption behavior and a marginally redshifted absorption maximum. This work shed light on spiro-fused nanographene structures with modulated optical and electronic properties.

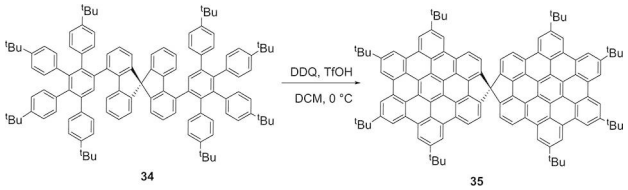

Scheme 14. Synthesis of compound **35** via oxidative cyclodehydrogenation.

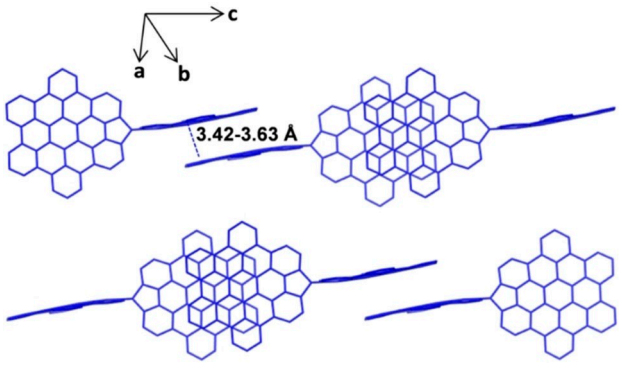

Figure 5. Molecular packing of compound **35** in a one-unit cell. Reproduced from reference [34] with permission from the Royal Society of Chemistry.

4. Rigid π systems with heteroatoms

Synthetic approaches have been developed to obtain spiro-compounds with incorporated heteroatoms to manipulate the optical, electrochemical, and charge-transport properties of the materials.

Perylene diimides (PDIs) are increasingly attracting academic attention aimed at desirable functionality for various optoelectronic devices. Wang et al. conducted a research milestone with the development of a straightforward palladium-catalyzed synthesis protocol toward spiro-fused electron-deficient moieties, such as spirodiperylenetetraimide (compound **37**) and PDI tetramer (compound **39**) shown in Scheme 15.[40] Surprisingly, in comparison with the parent PDI, the absorption maximum of compound **37** was significantly redshifted by ~23 nm (Figure 6), because of the distinct spiro-conjugation effect (which is imperceptible in other spiro-fused systems). Remarkably, the molar extinction coefficient of compound **39** peaked at 143400 $M^{-1}cm^{-1}$. Eventually, PDI and compound **37**/**39** - based non-fullerene photovoltaic devices (with the ITO/BHJ/M_oO_x/Al structure) produced power conversion efficiencies of 2.50%, 5.18%, and 7.17%, respectively. Thus, such spiro-fused PDI systems are regarded as a new type of high-performance semiconductor.

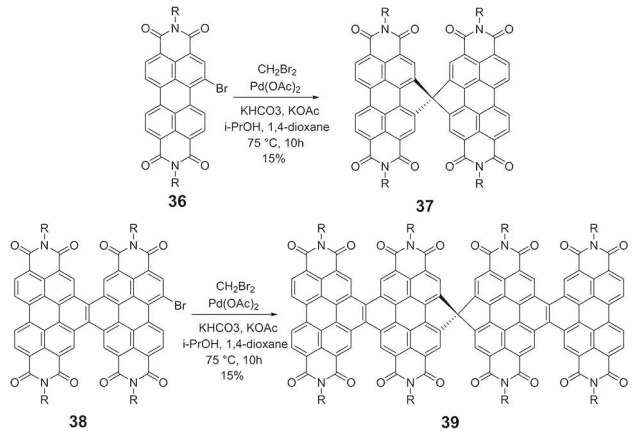

Scheme 15. Synthesis of spiro-fused perylene diimide compound **37** and derivative compound **39**.

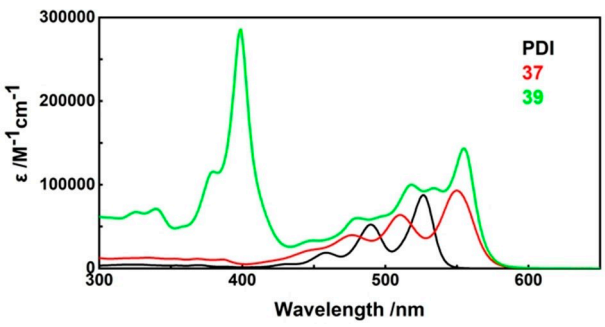

Figure 6. UV/vis absorption spectra of PDI (black), compound **37** (red), and compound **39** (green) in $CHCl_3$. Reproduced from reference [38] with permission from the American Chemical Society.

Recently, Wang et al. developed the first spiro-fused terrylene diimide (TDI)-based near-infrared circularly polarized luminescent (CPL) dye (compound **42**, Scheme 16).[41] Its R-and S-enantiomers were isolated by chiral high-performance liquid chromatography. Their CPL signals were mirror-images and covered the red and near-infrared regions, demonstrating their application potential in chiral optoelectronic devices or bio-imaging. Compound **42** further exhibited a considerably high molar extinction coefficient of 196700 M^{-1} cm^{-1} at 673 nm and a distinct redshift of 24 nm (in reference to compound **40**), due to the spiro-conjugation effect. Note that compound **42** possessed a lower PLQY (13%) compared with TDI (PLQY = 55%).

4,4-Difluoro-4-bora-3a,4a-diaza-s-indacenes (BODIPY) constitute advantageous fluorescent dyes because of their remarkable physical properties. Ohe et al. prepared structurally constrained BODIPY dyes based on spiro[fluorene-9,4(1H)-indeno[1,2-b]pyrrole][42–43] which exhibited a significantly increased PLQY, along with redshifted absorption and emission maxima (compared with non-spiro-fused counterparts). Because of the enhanced electron-donating abilities of methoxy and N,N-dimethylamino groups, compounds **43** and **44** (Scheme 17) exhibited bathochromic shifts of approximately 30 nm and 80 nm, respectively. More intriguingly, amino-substituted BODIPY dye compound **44** exhibited apparent intramolecular charge transfer characteristics, as confirmed by the fluorescence titration experiments.

Another series of rigid spiro-fused boron (III) compounds was designed and synthesized by Yam et al. in 2016.[44] By varying the substituents on the pyridine ring and extending the π-conjugation of the spiro framework, the emission color of these compounds could be adjusted to span the visible spectrum from blue to red. These compounds demonstrated an increased PLQY of up to 81% in CH_2Cl_2 solution. Solution-processed EL devices based on compounds **46**, **49**, and **52** (Scheme 18) were fabricated, in which an EQE of merely 1.3% with tunable emission color from red, to green, to blue was realized.

A new family of chiral spiro-fused aromatic compounds with thiophene units was synthesized by Nakano et al. in 2017 (Scheme 19).[45] Compound **53** could be oxidized to compounds **54** and **55** by meta-chlorperoxybenzoic acid (*m*CPBA) with 2.0 and 10 equiv., respectively. It is noteworthy that the PLQY of compound **55** (76%) was considerably higher than compound **53** (6%). As predicted, compound **55** presented significantly higher PLQY than its model compound **58**, whereas compound **53** possessed a lower PLQY than its model compound **59**. This inverse relationship is, however, unclear yet. Furthermore, compounds **54** and **55** could be converted to pyrrole-containing chiral spiro π-conjugated compounds **56** and **57**, respectively.[46] Due to the spiro-conjugation effect, compounds **53**, **55**, and **57** exhibited a redshifted spectrum compared to their model substructures **58**, **59**, and **60**, respectively. The

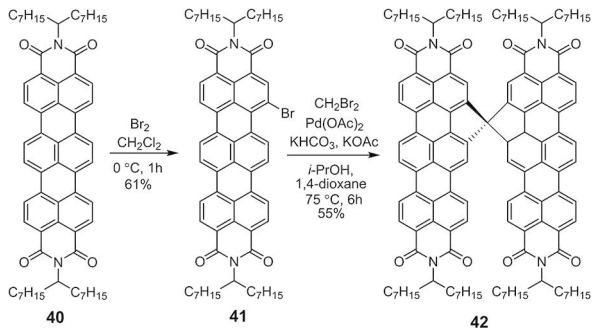

Scheme 16. Synthesis of spiro-fused terrylene diimide compound **42**.

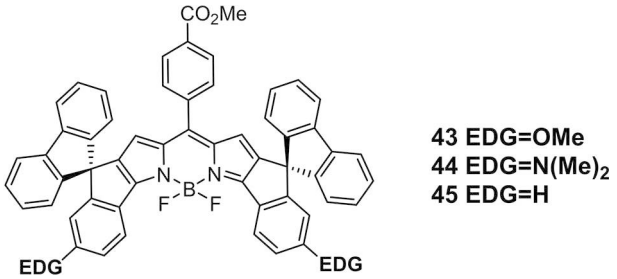

Scheme 17. Chemical structures of compounds **43**–**45**.

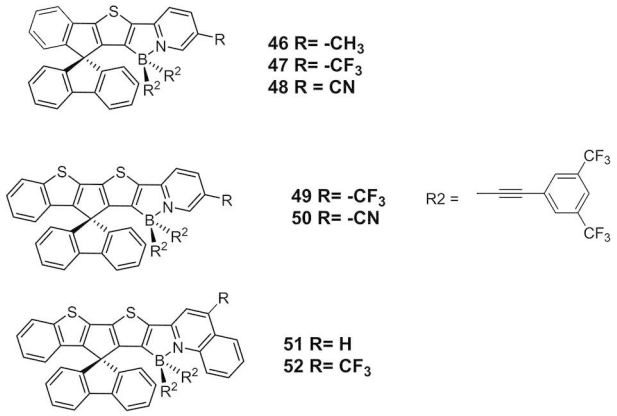

Scheme 18. Chemical structures of compounds **46**–**52**.

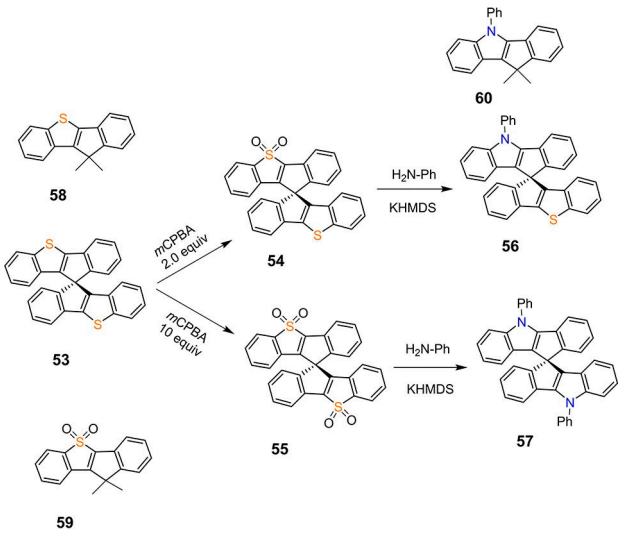

Scheme 19. Chemical structures of compounds **53**–**60**.

pyrrole-containing compounds **57** and **60** presented redshifted spectra compared with their thiophene equivalents, **53** and **58**. Notably, compounds **54** and **56** were the only to exhibit intramolecular charge transfer characteristics, thus resulting in a significantly low PLQY of 1% and 2%, respectively.

To enlarge the scope of spiro-fused compounds for electronics, Poriel et al. developed spiro fluorene xanthene (SFX) derivatives **61** and **62** (Scheme 20) with remarkable PLQYs of 63% and 91%, respectively.[47–49] The Stokes shifts of both **61** and **62** compounds were 3 and 4 nm, respectively. In comparison with their **1** and **14** carbon equivalents (respectively), compounds **61** and **62** presented analogous gaps and frontier orbital energy levels, demonstrating that the primary properties of these systems are induced by their corresponding central cores. The nonoptimized compound **61**-based OLED produced a brightness of approximately 3800 Cdm^{-2} and a maximum LE of 1 CdA^{-1}. Similarly, the compound **62**-based device reached a brightness of approximately 1400 Cdm^{-2} with a maximum LE of 0.35 CdA^{-1}. Compounds **61** and **62** were, thus, proven as beneficial emissive layers for OLEDs.

In 2016, Poriel et al. first incorporated thioxanthene and dioxothioxanthene moieties into the indeno[2,1-b]fluorene fragment to form compounds **63** and **64**[50] (Scheme 21); which possess notably similar absorption spectra, along with 2 nm redshifts in relation to difluorene-substituted indeno[2,1-b] fluorene (compound **17**). The incorporation of sulfur atoms in such molecular structures allows the manipulation of HOMO and LUMO energy levels, while retaining the high E_T of the dihydroindeno[2,1-b]fluorenyl core. Compound **64** was employed as a host in green and blue OLEDs with an EQE of 12.8% and 4.8%, respectively. In 2017, Xia et al. synthesized tetraindeno-fused spirofluorene-based blue emitter compounds **65** and **66**, which presented almost identical absorption spectra.[51] Single crystals were obtained via slow evaporation of tetrahydrofuran and ethyl acetate mixed solution for compound **65**, and tetrachloroethane solution for compound **66**. The distance between sulfur atoms of two neighboring molecules in compound **65** was shorter than their Van der Waals radii sum (1.85 Å). In the case of dioxothioxanthene compound **66**, no sulfur atom interactions were observed due to the bulky oxygen atoms.

To develop n-type 2D face-to-face π-stacking molecules, Xia et al. developed a method for annulated dicyano vinylene-substituted indeno-fused spirobifluorene.[52–53] Thereby, compounds **67** and **68** (Scheme 22) molecules were obtained via Knoevenagel condensation of the corresponding ketone precursors with Lehnert reagent, with yields of 99% and 90%, respectively. Both compounds exhibited a cruciform structure and underwent a 2D π-π stacking mode. Compound **68** possessed a significantly low LUMO energy of −3.76 eV. As illustrated in Figure 7, single crystals of compound **68** are highly expected to provide 2D electron transport along the π-stacking axes.

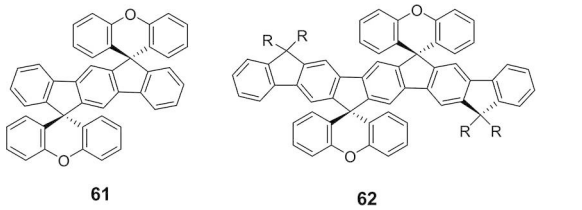

Scheme 20. Chemical structures of compounds **61** and **62**.

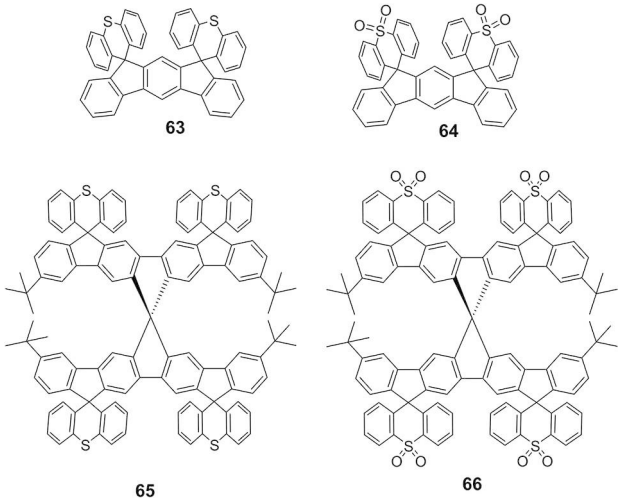

Scheme 21. Chemical structures of compounds **63**–**66**.

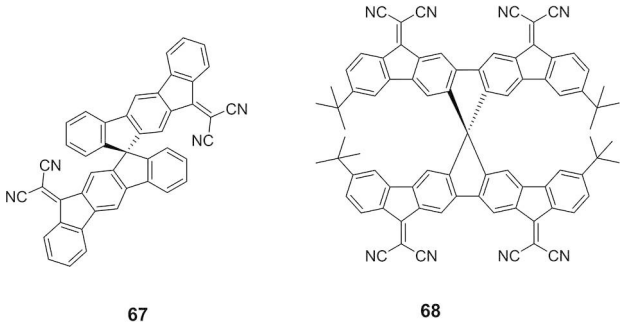

Scheme 22. Chemical structures of compounds **67** and **68**.

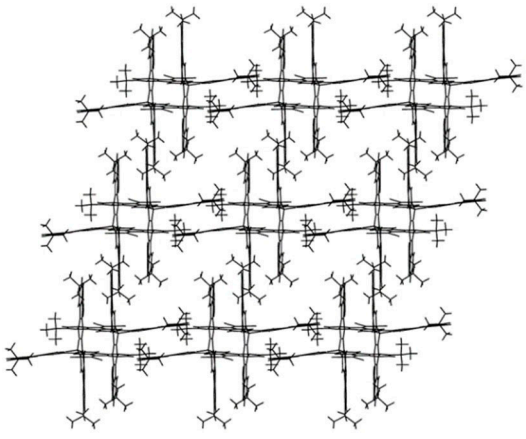

Figure 7. Molecular stacking patterns of compound **68**. Reproduced from reference [51] with permission from the American Chemical Society.

In 2006, Xie et al. designed and synthesized compound **69**[54] (Scheme 23) which is a novel dispiro building component for constructing H-shaped enduring architectures. Compound **69** displayed a maximum emission wavelength of 350 nm. In 2009, Ohe et al. reported another type of dispiro-fused system with O (**70**), S (**71**), and N (**72**) heteroatoms[55] (Scheme 23). The maximum emission peak of compound **71** was redshifted by approximately 40 nm in relation to compound **69**, indicating the considerable influence of the varying directions of thiophene ring substitutions on the effective conjugation.

In 2009, Liu et al. designed and synthesized the blue-emitter compound **73** (Scheme 24), which possessed a bent ladder-type hexaphenylene, a carbazole core, and a spiro-linkage.[56] Compound **73** exhibited an increased thermal decomposition temperature of 510 °C and a remarkably high glass-transition temperature (T_g) of 319 °C. A simple compound **73**-based OLED exhibited a maximum CE of 1.46 CdA^{-1} and a maximum LE of 505 cdm^{-2}.

In 2005, Yamaguchi et al. developed the spiro-fused compound **74**, composed of ladder oligo(-phenylenevinylene)s with

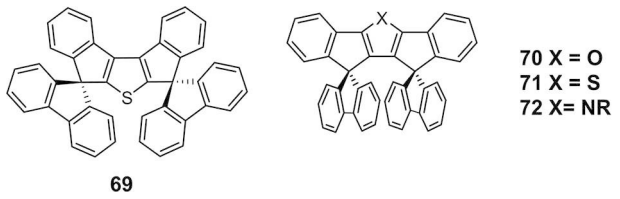

Scheme 23. Chemical structures of compounds **69**–**72**.

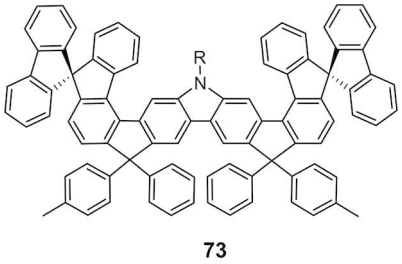

Scheme 24. Chemical structure of compound **73**.

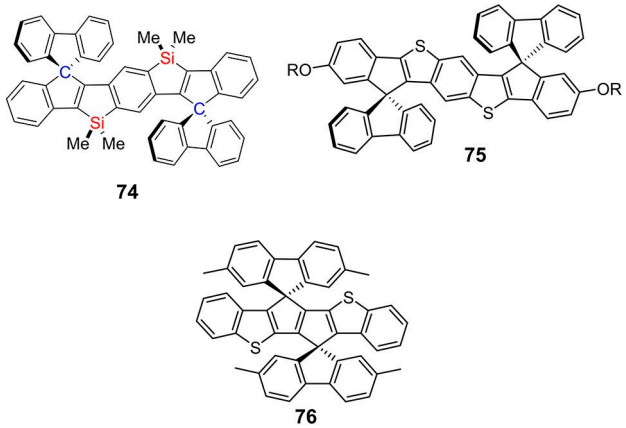

Scheme 25. Chemical structures of compounds **74**–**76**.

silicon and carbon bridges (Scheme 25).[57] In the same year, Pei et al. reported compound **75** with a unique linear sulfur-incorporated fused polycyclic aromatic, which presented interesting optical properties.[58] Its maximum absorption and emission peaks were observed at 406 and 421 nm, respectively. In 2015, Jin et al. reported a $FeCl_3$-mediated oxidative spirocyclization method for the construction of a new class of di-spiro linked π-conjugated molecules. Consequently, compound **76** with thiophene rings could be obtained in 95% yield at room temperature.[34]

5. Rigid Polymers

In 2008, Bo et al. reported a spirobifluorene-based rigid polymer **78**[59] which was prepared via treatment of polymer **77** with a catalytic amount of BF_3•etherate, in 90% yield (Scheme 26). Owing to its rigid conjugated backbone, polymer **78** presented unique properties such as a remarkably high decomposition temperature (435 °C), a tiny Stokes shift (2 nm), and excellent optical stability. It is noteworthy that no essential shift of the UV and PL spectra from solution to film occurred, since the three-dimensional spirobifluorene units were pivotal in suppressing the aggregation of polymer chains. Beneficially, the EL spectrum of the polymer **78**-based OLED was essentially identical to the PL spectrum, and no ketonic defects on the polymer chains were detected.

Neil B. McKeown et al. reported a rigid polymer **80**,[60] which was synthesized via aromatic nucleophilic substitution reaction (Scheme 27). Polymer **80** demonstrated greater selectivity than ordinary polymers, without loss of permeability. The improved performance of polymer **80** was attributed to its enhanced rigidity. Mixed CO_2/CH_4 gas permeation measurements for aged polymer **80** further demonstrated its potential for natural gas and/or biogas upgrading.

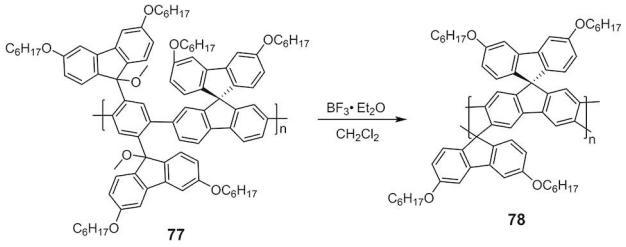

Scheme 26. Synthesis of compound **78** via cyclization reaction from compound **77**.

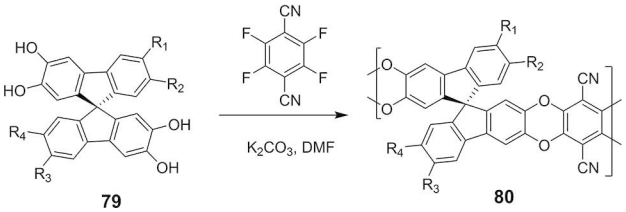

Scheme 27. Synthesis of compound **80** via aromatic nucleophilic substitution reaction.

Takata et al. developed a method to synthesize helical polymers based on rigid C_2-chial repeating units.[61] In 2015, they constructed a coil-shaped compound **82** and screw-shaped compound **84** (Scheme 28), with rigid structures, via reductive cyclization reactions. Surprisingly, the two polymers were highly soluble in water, since sulfonation might occur on the fluorene moieties. This behavior facilitates the investigation of optical properties in solution. These helical polymers could potentially be employed as chiral sensors and chiral catalysts.

6. Multiple single-bond-linked rigid spiro-bifluorenes or π-systems

Recently, Toru Amaya et al. reported single-bond linked rigid dimeric spirobifluorenes (compound **85**) and trimeric spirobifluorenes (compound **86**) presented in Scheme 29.[62] These structures resulted in the bending of oligophenylenes in the dimer, and the double S-shaped structure alignment in the trimer. Surprisingly, no (S,S or R,R)-compound **85** was detected, despite their significantly lower energy compared with (meso)-compound **85**. Regarding compound **86**, only (R,P,R/S,M,S)-compound **86** was formed and isolated (Figure 8); neither (R,M,R/S,P,S)-, nor (R,R,S/S,S,R)-compound **85** were detected, even after meticulous analyzation of the crude products. The absorption spectrum of (R,P,R/S,M,S)-compound **85** sustained bathochromic shifts of 25–50 nm (compared with their singly bonded trimeric counterparts), which was explained by the through-space interactions of molecular orbitals between two strands and confirmed by DFT computations. This chiral spirobifluorene linking strategy produced a variety of structurally rigid molecules with unique molecular geometries and properties.

In 2019, Miki et al. reported helically bridged conjugated spirobifluorenes.[63] These curved structures of phenylenethynyleneanthryl bridged spirobifluorene moieties with (S, S) and (R, R) chirality presented circular polarized luminescence. A remarkably increased quantum yield of 93% was reported in compound **87** (Scheme 30), with minimal structural change upon photoirradiation. In contrast, a carbon-based double-helicate counterpart, hinged by (S)-2,2′-diethynyl-1,1′-binaphthyl moieties, demonstrated dynamic structural changes under photoirradiation and the quantum yield was decreased to 49%. The notable difference in the photophysical properties between the two carbon-based double-helices compounds stemmed from their varying rigidities.

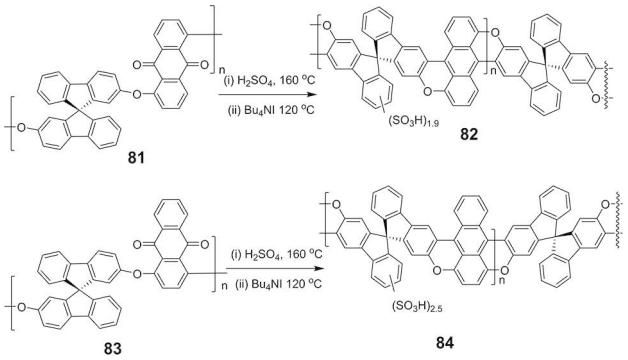

Scheme 28. Syntheses of coil-shaped compound **82** and screw-shaped compound **84**.

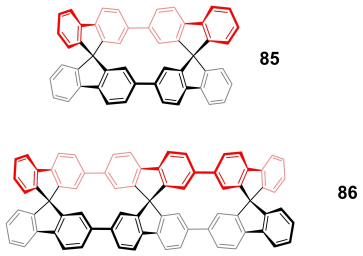

Scheme 29. Chemical structures of compounds **85** and **86**.

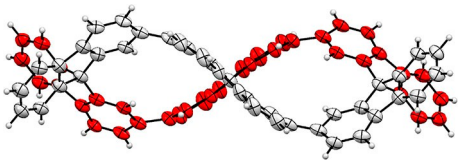

Figure 8. The molecular structure of compound **86** from single-crystal X-ray diffraction data. Reproduced from ref 59 with permission from the American Chemical Society.

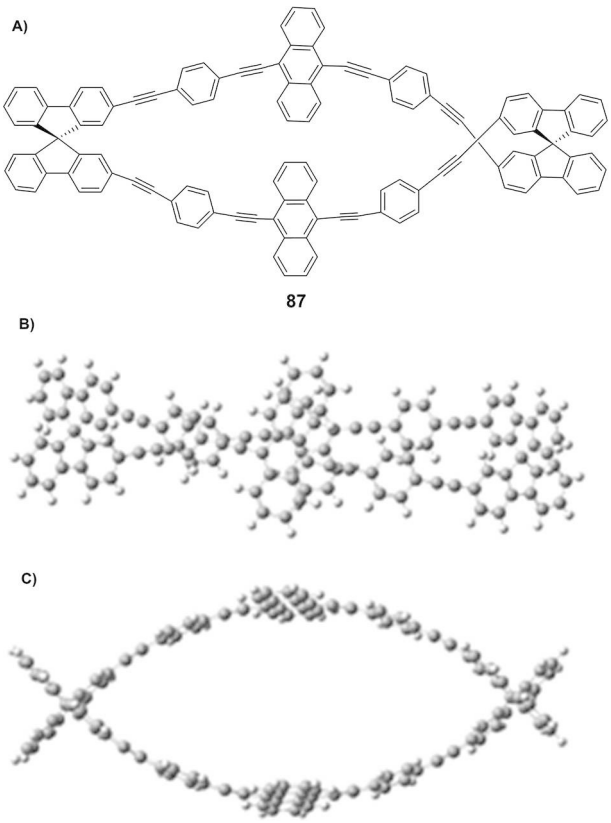

Scheme 30. Chemical structure of compound **87** with top, side, and below

7. Summary and Outlook

In conclusion, we have summarized the recent progress regarding spiro-conjugated and fused rigid π-systems originating from spiro-bifluorene and indeno fused compounds. Concerning their optical properties, these rigid π-systems typically possess high PLQYs and small Stokes shifts, which are highly beneficial/advantageous factors for increased color purity and applications in OLED devices (both as emitters and hole transporting materials). Recently, spiro linkages have been extended to form large polycyclic aromatic hydrocarbon compounds (such as hexabenzocoronene or perylene and terrylene diimides), presenting unique photophysical properties.

During the last few decades, material chemists have explored the functionalities of nanobelts and nanographene and how their material purities severely limited their device performance. In recent years, organic chemists have attempted to synthesize these compounds. For instance, Itami et al. fabricated a carbon nanobelt comprising of fused edge-sharing benzene rings.[64] Muellen et al. employed a bottom-up approach and synthesized structurally well-defined graphene nanoribbons.[65] Considering the above, combining spiro structures with carbon nanobelts and nanographene could potentially provide a functional solution, given the advanced 3D charge transport and thermal/electrical stability of these structures. Concludingly, the potential that spiro-linked rigid structures present in extending dimensionality, is expected to expand their applications in a wide range of technological areas.

Acknowledgements

This work was supported by the Max Planck Institute for Polymer Research, the National Natural Science Foundation of China (No. 51603055), Natural Science Foundation of Heilongjiang Province (No. QC2017055), the China Postdoctoral Science Foundation 2017T100236), and the Postdoctoral Foundation of Heilongjiang Province (Nos. LBH-Z16059 and LBH-TZ10). Open access funding enabled and organized by Projekt DEAL.

Conflict of Interest

The authors declare no conflict of interest.

Keywords: polycyclic aromatic hydrocarbons · spirobifluorenes · spiro-conjugation · spiro-fusion

[1] H. E. Simmons, T. Fukunaga, *J. Am. Chem. Soc.* **1967**, *89*, 5208–5215.
[2] T. P. I. Saragi, T. Spehr, A. Siebert, T. Fuhrmann-Lieker, J. Salbeck, *Chem. Rev.* **2007**, *107*, 1011–1065.
[3] C. Poriel, J. Rault-Berthelot, *Acc. Chem. Res.* **2018**, *51*, 1818–1830.
[4] R. Pudzich, T. Fuhrmann-Lieker, J. Salbeck in *Spiro Compounds for Organic Electroluminescence and Related Applications,* Springer Berlin Heidelberg, Berlin, Heidelberg, **2006**, pp.83–142.
[5] C. Poriel, L. Sicard, J. Rault-Berthelot, *Chem. Commun.* **2019**, *55*, 14238–14254.
[6] C. Poriel, J. Rault-Berthelot, *J. Mater. Chem. C.* **2017**, *5*, 3869–3897.
[7] X. Yang, X. Xu, G. Zhou, *J. Mater. Chem. C.* **2015**, *3*, 913–944.
[8] S. Shao, Z. Ma, J. Ding, L. Wang, X. Jing, F. Wang, *Adv. Mater.* **2012**, *24*, 2009–2013.
[9] J. Liu, S. Chen, D. Qian, B. Gautam, G. Yang, J. Zhao, J. Bergqvist, F. Zhang, W. Ma, H. Ade, O. Inganäs, K. Gundogdu, F. Gao, H. Yan, *Nat. Energy.* **2016**, *1*, 16089.
[10] S. Ma, Y. Fu, D. Ni, J. Mao, Z. Xie, G. Tu, *Chem. Commun.* **2012**, *48*, 11847–11849.
[11] X.-F. Wu, W.-F. Fu, Z. Xu, M. Shi, F. Liu, H.-Z. Chen, J.-H. Wan, T. P. Russell, *Adv. Funct. Mater.* **2015**, *25*, 5954–5966.
[12] Q. Yan, Y. Zhou, Y.-Q. Zheng, J. Pei, D. Zhao, *Chem. Sci.* **2013**, *4*, 4389–4394.
[13] J. Lee, R. Singh, D. H. Sin, H. G. Kim, K. C. Song, K. Cho, *Adv. Mater.* **2016**, *28*, 69–76.
[14] D. Horhant, J.-J. Liang, M. Virboul, C. Poriel, G. Alcaraz, J. Rault-Berthelot, *Org. Lett.* **2006**, *8*, 257–260.
[15] Y. Wu, J. Zhang, Z. Bo, *Org. Lett.* **2007**, *9*, 4435–4438.
[16] C. Poriel, J.-J. Liang, J. Rault-Berthelot, F. Barrière, N. Cocherel, A. M. Z. Slawin, D. Horhant, M. Virboul, G. Alcaraz, N. Audebrand, L. Vignau, N. Huby, G. Wantz, L. Hirsch, *Chem. Eur. J.* **2007**, *13*, 10055–10069.
[17] C. Poriel, J. Rault-Berthelot, F. Barrière, A. M. Z. Slawin, *Org. Lett.* **2008**, *10*, 373–376.
[18] D. Thirion, C. Poriel, F. Barrière, R. Métivier, O. Jeannin, J. Rault-Berthelot, *Org. Lett.* **2009**, *11*, 4794–4797.
[19] B. Kobin, J. Schwarz, B. Braun-Cula, M. Eyer, A. Zykov, S. Kowarik, S. Blumstengel, S. Hecht, *Adv. Funct. Mater.* **2017**, *27*, 1704077.
[20] N. Cocherel, C. Poriel, J. Rault-Berthelot, F. Barrière, N. Audebrand, A. M. Z. Slawin, L. Vignau, *Chem. Eur. J.* **2008**, *14*, 11328–11342.
[21] D. Xia, C. Duan, S. Liu, D. Ding, M. Baumgarten, M. Wagner, D. Schollmeyer, H. Xu, K. Müllen, *New J. Chem.* **2019**, *43*, 3788–3792.
[22] M. Romain, D. Tondelier, J.-C. Vanel, B. Geffroy, O. Jeannin, J. Rault-Berthelot, R. Métivier, C. Poriel, *Angew. Chem. Int. Ed.* **2013**, *52*, 14147–14151; *Angew. Chem.* **2013**, *125*, 14397–14401.
[23] M. Romain, S. Thiery, A. Shirinskaya, C. Declairieux, D. Tondelier, B. Geffroy, O. Jeannin, J. Rault-Berthelot, R. Métivier, C. Poriel, *Angew. Chem. Int. Ed.* **2015**, *54*, 1176–1180; *Angew. Chem.* **2015**, *127*, 1192–1196.
[24] D. Thirion, C. Poriel, J. Rault-Berthelot, F. Barrière, O. Jeannin, *Chem. Eur. J.* **2010**, *16*, 13646–13658.
[25] D. Thirion, C. Poriel, R. Métivier, J. Rault-Berthelot, F. Barrière, O. Jeannin, *Chem. Eur. J.* **2011**, *17*, 10272–10287.
[26] L. Zhao, C. Duan, D. Ding, S. Liu, D. Xia, Y. Guo, H. Xu, M. Baumgarten, *Chin. Chem. Lett.* **2020**.
[27] J. Ramakrishna, P. Venkatakrishnan, *Chem. Asian J.* **2017**, *12*, 181–189.
[28] N. Harada, H. Ono, T. Nishiwaki, H. Uda, *J. Chem. Soc. Chem. Commun.* **1991**, 1753–1755.
[29] S.-O. Jeon, Y.-M. Jeon, J.-W. Kim, C.-W. Lee, M.-S. Gong, *Org. Electron.* **2008**, *9*, 522–532.
[30] J.-R. Cha, C.-W. Lee, M.-S. Gong, *New J. Chem.* **2015**, *39*, 3813–3820.
[31] H. Lee, H. Jung, S. Kang, J. H. Heo, S. H. Im, J. Park, *J. Org. Chem.* **2018**, *83*, 2640–2646.
[32] Y. Sawada, S. Furumi, A. Takai, M. Takeuchi, K. Noguchi, K. Tanaka, *J. Am. Chem. Soc.* **2012**, *134*, 4080–4083.
[33] K. Murayama, Y. Shibata, H. Sugiyama, H. Uekusa, K. Tanaka, *J. Org. Chem.* **2017**, *82*, 1136–1144.
[34] J. Zhao, Z. Xu, K. Oniwa, N. Asao, Y. Yamamoto, T. Jin, *Angew. Chem. Int. Ed.* **2016**, *55*, 259–263; *Angew. Chem.* **2016**, *128*, 267–271.
[35] H. Hamada, Y. Itabashi, R. Shang, E. Nakamura, *J. Am. Chem. Soc.* **2020**, *142*, 2059–2067.
[36] M. Kimura, S. Kuwano, Y. Sawaki, H. Fujikawa, K. Noda, Y. Taga, K. Takagi, *J. Mater. Chem.* **2005**, *15*, 2393–2398.
[37] T. Lei, J. Luo, L. Wang, Y. Ma, J. Wang, Y. Cao, J. Pei, *New J. Chem.* **2010**, *34*, 699–707.
[38] A. M. v. d. Craats, J. M. Warman, A. Fechtenkötter, J. D. Brand, M. A. Harbison, K. Müllen, *Adv. Mater.* **1999**, *11*, 1469–1472.
[39] Y. Hu, D. Wang, M. Baumgarten, D. Schollmeyer, K. Müllen, A. Narita, *Chem. Commun.* **2018**, *54*, 13575–13578.
[40] G. Gao, N. Liang, H. Geng, W. Jiang, H. Fu, J. Feng, J. Hou, X. Feng, Z. Wang, *J. Am. Chem. Soc.* **2017**, *139*, 15914–15920.
[41] J. Feng, L. Fu, H. Geng, W. Jiang, Z. Wang, *Chem. Commun.* **2020**, *56*, 912–915.
[42] T. Kowada, S. Yamaguchi, K. Ohe, *Org. Lett.* **2010**, *12*, 296–299.

[43] T. Kowada, S. Yamaguchi, H. Fujinaga, K. Ohe, *Tetrahedron.* **2011**, *67*, 3105–3110.
[44] B. Y.-W. Wong, H.-L. Wong, Y.-C. Wong, M.-Y. Chan, V. W.-W. Yam, *Chem. Eur. J.* **2016**, *22*, 15095–15106.
[45] K. Takase, K. Noguchi, K. Nakano, *Org. Lett.* **2017**, *19*, 5082–5085.
[46] K. Takase, K. Noguchi, K. Nakano, *Bull. Chem. Soc. Jpn.* **2019**, *92*, 1008–1017.
[47] N. Cocherel, C. Poriel, L. Vignau, J.-F. Bergamini, J. Rault-Berthelot, *Org. Lett.* **2010**, *12*, 452–455.
[48] H. Mokbel, C. Poriel, J. Rault-Berthelot, F. Dumur, D. Gigmes, J. Toufaily, T. Hamieh, D. Cordella, C. Detrembleur, J. P. Fouassier, J. Lalevée, *J. Appl. Polym. Sci.* **2016**, *133*.
[49] C. Poriel, N. Cocherel, J. Rault-Berthelot, L. Vignau, O. Jeannin, *Chem. Eur. J.* **2011**, *17*, 12631–12645.
[50] M. Romain, C. Quinton, D. Tondelier, B. Geffroy, O. Jeannin, J. Rault-Berthelot, C. Poriel, *J. Mater. Chem. C.* **2016**, *4*, 1692–1703.
[51] J. Guan, F. Zhang, Y. Zhang, Z. Liu, Y. Wu, D. Xia, *CrystEngComm.* **2017**, *19*, 6752–6757.
[52] D. Xia, D. Gehrig, X. Guo, M. Baumgarten, F. Laquai, K. Müllen, *J. Mater. Chem. A* **2015**, *3*, 11086–11092.
[53] D. Xia, X. Guo, M. Wagner, M. Baumgarten, D. Schollmeyer, K. Müllen, *Cryst. Growth Des.* **2017**, *17*, 2816–2821.
[54] L.-H. Xie, X.-Y. Hou, C. Tang, Y.-R. Hua, R.-J. Wang, R.-F. Chen, Q.-L. Fan, L.-H. Wang, W. Wei, B. Peng, W. Huang, *Org. Lett.* **2006**, *8*, 1363–1366.
[55] T. Kowada, T. Kuwabara, K. Ohe, *J. Org. Chem.* **2010**, *75*, 906–913.
[56] Z. Jiang, H. Yao, Z. Liu, C. Yang, C. Zhong, J. Qin, G. Yu, Y. Liu, *Org. Lett.* **2009**, *11*, 4132–4135.
[57] C. Xu, A. Wakamiya, S. Yamaguchi, *J. Am. Chem. Soc.* **2005**, *127*, 1638–1639.
[58] C.-H. Wang, R.-R. Hu, S. Liang, J.-H. Chen, Z. Yang, J. Pei, *Tetrahedron Lett.* **2005**, *46*, 8153–8157.
[59] Y. Wu, J. Zhang, Z. Fei, Z. Bo, *J. Am. Chem. Soc.* **2008**, *130*, 7192–7193.
[60] C. G. Bezzu, M. Carta, M.-C. Ferrari, J. C. Jansen, M. Monteleone, E. Esposito, A. Fuoco, K. Hart, T. P. Liyana-Arachchi, C. M. Colina, N. B. McKeown, *J. Mater. Chem. A* **2018**, *6*, 10507–10514.
[61] Z. Yi, H. Okuda, Y. Koyama, R. Seto, S. Uchida, H. Sogawa, S. Kuwata, T. Takata, *Chem. Commun.* **2015**, *51*, 10423–10426.
[62] J. Oniki, T. Moriuchi, K. Kamochi, M. Tobisu, T. Amaya, *J. Am. Chem. Soc.* **2019**, *141*, 18238–18245.
[63] K. Miki, T. Noda, M. Gon, K. Tanaka, Y. Chujo, Y. Mizuhata, N. Tokitoh, K. Ohe, *Chem. Eur. J.* **2019**, *25*, 9211–9216.
[64] G. Povie, Y. Segawa, T. Nishihara, Y. Miyauchi, K. Itami, *Science.* **2017**, *356*, 172–175.
[65] A. Narita, X. Feng, Y. Hernandez, S. A. Jensen, M. Bonn, H. Yang, I. A. Verzhbitskiy, C. Casiraghi, M. R. Hansen, A. H. R. Koch, G. Fytas, O. Ivasenko, B. Li, K. S. Mali, T. Balandina, S. Mahesh, S. De Feyter, K. Müllen, *Nat. Chem.* **2014**, *6*, 126–132.

Manuscript received: June 15, 2020
Revised manuscript received: August 24, 2020
Accepted manuscript online: August 24, 2020